Cell Host & Microbe
Article

A Malaria Parasite Formin Regulates Actin Polymerization and Localizes to the Parasite-Erythrocyte Moving Junction during Invasion

Jake Baum,[1] Christopher J. Tonkin,[1,7] Aditya S. Paul,[4,7] Melanie Rug,[1] Brian J. Smith,[2] Sven B. Gould,[3] Dave Richard,[1] Thomas D. Pollard,[4,5,6] and Alan F. Cowman[1,*]
[1]Infection and Immunity Division
[2]Structural Biology Division
The Walter and Eliza Hall Institute of Medical Research, Parkville, Victoria 3050, Australia
[3]School of Botany, University of Melbourne, Melbourne, Victoria 3010, Australia
[4]Department of Molecular Biophysics and Biochemistry
[5]Departments of Molecular, Cellular, and Developmental Biology
[6]Department of Cell Biology
Yale University, New Haven, CT 06510, USA
[7]These authors contributed equally to this work.
*Correspondence: cowman@wehi.edu.au
DOI 10.1016/j.chom.2008.02.006

SUMMARY

Malaria parasites invade host cells using actin-based motility, a process requiring parasite actin filament nucleation and polymerization. Malaria and other apicomplexan parasites lack Arp2/3 complex, an actin nucleator widely conserved across eukaryotes, but do express formins, another type of actin nucleator. Here, we demonstrate that one of two malaria parasite formins, *Plasmodium falciparum* formin 1 (PfFormin 1), and its ortholog in the related parasite *Toxoplasma gondii*, follows the moving tight junction between the invading parasite and the host cell, which is the predicted site of the actomyosin motor that powers motility. Furthermore, in vitro, the PfFormin1 actin-binding formin homology 2 domain is a potent nucleator, stimulating actin polymerization and, like other formins, localizing to the barbed end during filament elongation. These findings support a conserved molecular mechanism underlying apicomplexan parasite motility and, given the essential role that actin plays in cell invasion, highlight formins as important determinants of malaria parasite pathogenicity.

INTRODUCTION

The phylum Apicomplexa comprises a group of single-celled, early branching eukaryotes that includes malaria parasites and other pathogenic protozoa of humans and livestock. Instead of using either cilia or flagella (based on microtubule axonemes) or actin assembly driven by Arp2/3 complex to move, apicomplexan parasites use a unique actomyosin-based, substrate-dependent form of locomotion, called gliding motility, to cross epithelial barriers and invade target host cells (Baum et al., 2006a; Morrissette and Sibley, 2002). The molecular motor, thought to drive this process, is housed in a space (referred to as the supra-alveolar space) (Raibaud et al., 2001) within the parasite pellicle that lies between the outer plasma membrane and the inner membrane complex (Baum et al., 2006a; Morrissette and Sibley, 2002). The motor consists of a single-headed myosin found only in Apicomplexa (Foth et al., 2006; Meissner et al., 2002) that tread along short, dynamic, actin filaments (Sahoo et al., 2006; Schmitz et al., 2005; Schuler et al., 2005). Myosin is anchored in the external face of the inner membrane complex (Gaskins et al., 2004), while actin filaments, lying within the supra-alveolar space (Dobrowolski et al., 1997; Patron et al., 2005; Shaw and Tilney, 1999; Wetzel et al., 2003), form a bridge with the extra-cellular environment via the cytoplasmic tail of transmembrane-bound adhesins secreted onto the parasite surface (Baum et al., 2006b; Jewett and Sibley, 2003). The binding of these adhesins to the host surface and their rearward movement, driven by myosin via actin, propels the parasite over the cell substratum or powers active penetration of target cells (reviewed in Baum et al., 2006a). It has been known for some time that drugs that disrupt actin polymerization or filament turnover block motility and cell invasion of apicomplexan parasites, demonstrating the essential role of dynamic actin (Dobrowolski and Sibley, 1996; Miller et al., 1979; Mizuno et al., 2002; Pinder et al., 1998; Wetzel et al., 2003). However, the cellular factors regulating actin in Apicomplexa and the signal cascades that lead to polymerization are mostly unknown.

Apicomplexa lack genes for many known actin regulators (Baum et al., 2006a), including the subunits of Arp2/3 complex, which nucleates actin filaments in plants, amoebas, fungi, and animals (Pollard, 2007). Apicomplexa do have genes for formins (Goode and Eck, 2007; Pollard, 2007), a family of proteins that nucleate unbranched actin filaments for many structures across eukaryotes (Higashida et al., 2004; Martin and Chang, 2006; Michelot et al., 2005; Sagot et al., 2002). The defining feature of formin proteins is the formin homology (FH) 2 domain (Higgs and Peterson, 2005), a region of ~400 amino acids that forms

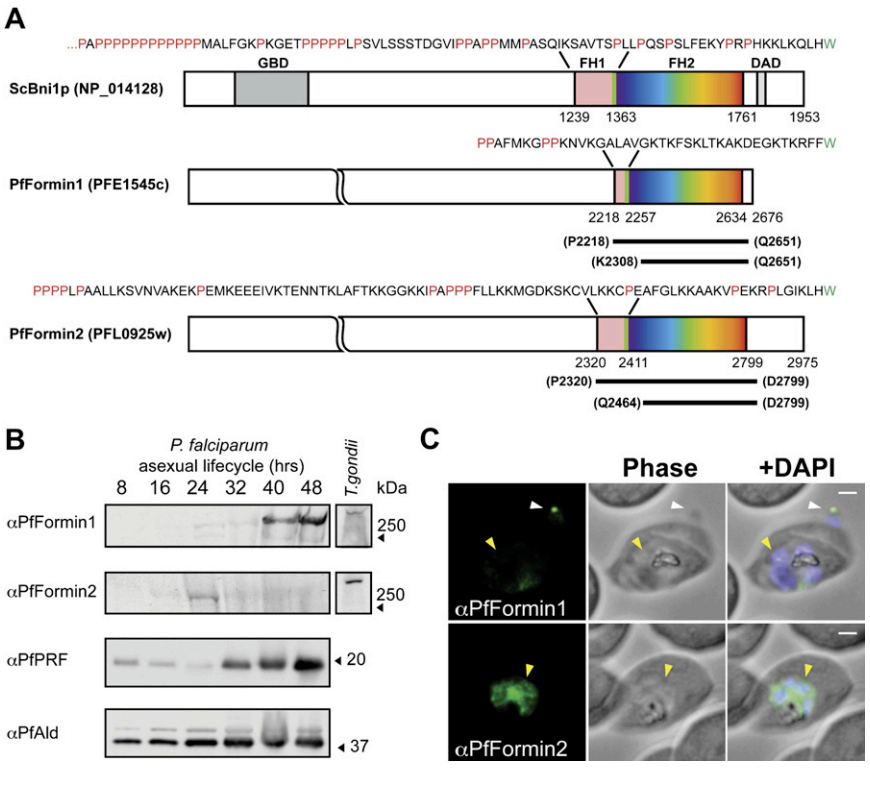

Figure 1. *Plasmodium falciparum* Expresses Two Formins

(A) Schematic representation of *S. cerevisiae* formin Bni1p and *P. falciparum* formins. FH2 domain coloring correlates with the structural model (Figure S3). Numbers below protein schematic indicate amino acid residue derived from reference sequences. Black lines designate constructs used in this study. Expanded sequences upstream of the key tryptophan (W) residue represent putative formin homology (FH)-1 domains with proline (P) residues marked in red. Neither *P. falciparum* formin contain any of the other well-characterized regulatory domains including the GTPase-binding (GDB) and diaphanous auto-regulatory (DAD) domains found in formins like Bni1p.

(B) *P. falciparum* formins are expressed differentially. Immunoblot of whole *P. falciparum* parasite lysate at 8 hr intervals across the 48 hr lifecycle (0 hr, invasion) and whole *T. gondii* parasite lysate (last lane) probed with polyclonal rabbit antiserum raised against recombinant FH2 domains of PfFormin1 and PfFormin2 and recombinant PfPRF (rabbit anti-PfAldolase, loading control).

(C) Immunofluorescence and phase contrast micrographs of asexual blood-stage *P. falciparum* parasites stained with the same PfFormin1 or PfFormin2 antisera. Yellow arrows point to periphery of intraerythrocytic trophozoite. White arrows point to apical pole of merozoite. DAPI nuclear stain. Scale bar, 1 μM.

a homodimer (Otomo et al., 2005; Xu et al., 2004), which typically remains bound to the growing barbed end of a nucleated filament (Higashida et al., 2004; Kovar et al., 2006; Romero et al., 2004). Most formins also contain a proline-rich FH1 domain adjacent to the FH2 domain (Higgs and Peterson, 2005), which binds profilin-actin complexes for efficient delivery of new monomers onto growing filaments (Kovar et al., 2006; Kovar et al., 2003; Paul and Pollard, 2008; Romero et al., 2004). A search for predicted proteins containing regions homologous to the FH2 domain of the budding yeast formin Bni1p (residues 1348-1766) (Higgs and Peterson, 2005) in the genome sequence of *Plasmodium falciparum*, the most virulent human malaria parasite, previously identified two very large (>300 kDa) formin-like proteins (Baum et al., 2006a), here called *P. falciparum* formin 1 (PfFormin1) and formin 2 (PfFormin2) (Figure 1A) (previously called PfForB and PfForA, respectively [Baum et al., 2006a]). The genomes of other apicomplexan parasites, including several malaria parasite species, also contain orthologs of 1- and 2-like formins (Baum et al., 2006a). These cluster into two distinct families (see Figure S1 available online), suggesting that each formin may play a conserved role in actin regulation.

Here, we show that of the two formins expressed in *P. falciparum*, PfFormin1 localizes precisely with the predicted location of the activated actomyosin motor in invading malaria parasites and is a potent nucleator of actin filaments in vitro. Furthermore, we show that the formin 1 ortholog in *Toxoplasma gondii* follows a similar localization during host cell invasion, supporting the notion that motility across apicomplexan parasites is governed by conserved molecular mechanisms. Given the essential role that actin plays in cell invasion, formin 1 as an actin regulator represents a potential key effector of host cell invasion and, as such, of parasite pathogenicity.

RESULTS

Differential Expression and Localization of Malaria Parasite Formins 1 and 2

Microarray data through the lifecycle of the malaria parasite, *P. falciparum*, suggests that the two formins are expressed across asexual and sexual stages of development (Le Roch et al., 2003). To definitively determine their presence in the erythrocytic stages (the lifecycle stage associated with disease) we raised antibodies against recombinant FH2 domains for both *P. falciparum* formins (Figure 1A). Immunoblots demonstrate that both are expressed during asexual parasite development (Figure 1B). In agreement with its gene expression profile (Le Roch et al., 2003), maximal expression of PfFormin1 is late in the lifecycle at 40–48 hr postinvasion (Figure 1B), a stage when much of the machinery for erythrocyte invasion is assembled. Immunofluorescence microscopy of free merozoites demonstrates that PfFormin1 concentrates at the tip of the parasite (Figure 1C; white arrow) while being absent from earlier trophozoites (Figure 1C; yellow arrow). In contrast, PfFormin2 expression peaks 24 hr postinvasion at the mid trophozoite stage (Figure 1B), a time of parasite growth and nuclear division and, by immunofluorescence, localizes diffusely through the trophozoite cell cytoplasm though largely absent from the nucleus (Figure 1C). Given its pattern of expression and anterior localization we colocalized PfFormin1 with other components known to be important to cell invasion. Immunofluorescence clearly shows

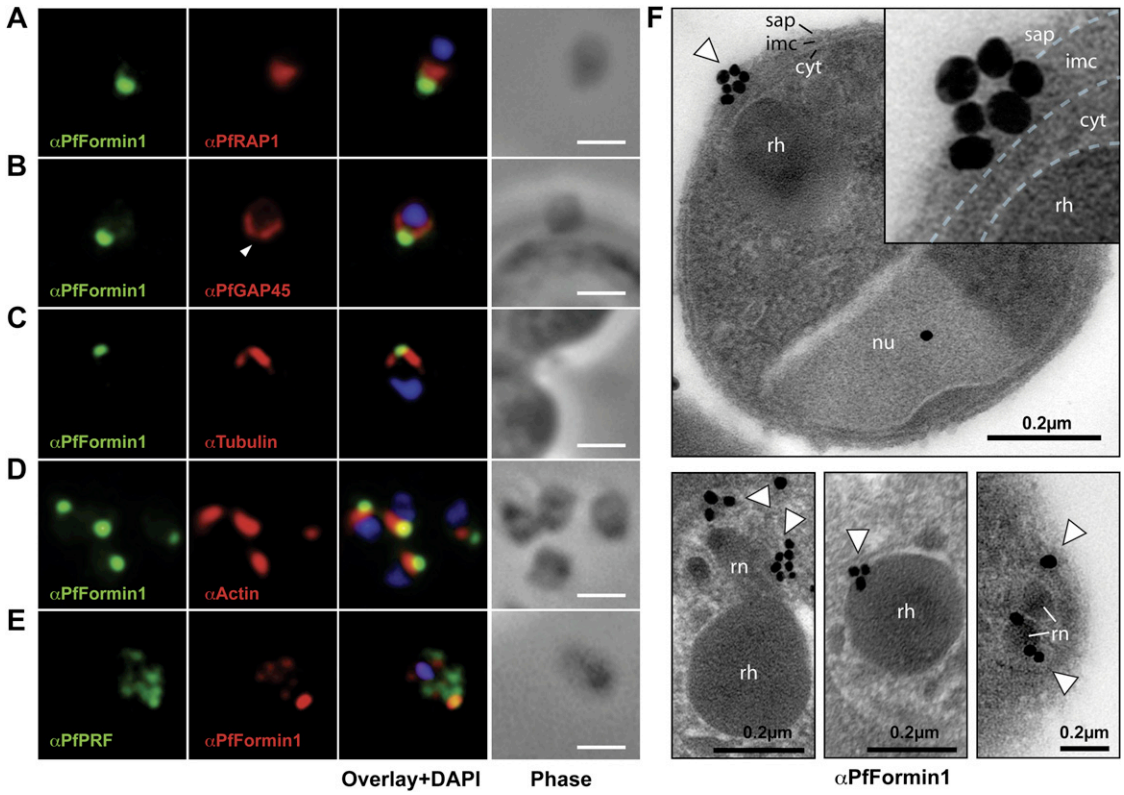

Figure 2. PfFormin1 Localizes at the Apical Pole of Free Merozoites

Immunofluorescence and phase contrast micrographs of free merozoites postschizont rupture. Immunofluorescent colocalization of rabbit anti-PfFormin1 with various merozoite organelle components using mouse antisera against (A) PfRAP1, a protein found within the apical secretory organelles (the rhoptries) of merozoites; (B) PfGAP45, a key constituent of the invasion motor that localizes to the inner membrane complex but is absent from the extreme apical tip (white arrow); (C) tubulin, a component of the subpellicular microtubules; and (D) actin. (E) Colocalization of rabbit anti-PfPRF with mouse antisera against PfFormin1. DAPI nuclear stain. Scale bars, 1 μM. (F) Immunoelectron micrographs showing localization of formin 1 in late schizonts of *P. falciparum* 3D7 with 25-nm-diameter colloidal gold. Labeling is concentrated at the apical pole anterior to the rhoptry body (rh) and neck (rn). Close inspection of the three pellicular membranes (inset) suggests labeling is concentrated at the break in the inner membrane complex (imc) possibly associated with the supra-alveolar space (sap). Other labels mark the cytosol (cyt) and nucleus (nu).

that it resides at the apical pole of free merozoites in front of the bulb of the rhoptry (an apical organelle involved in invasion) (Figure 2A) and anterior to the natural apical break in the inner membrane complex (Figure 2B; white arrow) (Morrissette and Sibley, 2002). This location coincides with the apical polar rings and the microtubule-organizing center from which the limited number of merozoite microtubules originate (Morrissette and Sibley, 2002) (Figure 2C). The region anterior to the apical pole is also the area where actin appears to be concentrated (Figure 2D) (Mizuno et al., 2002; Shaw and Tilney, 1999; Wetzel et al., 2003). Immunoelectron microscopy of free merozoites using anti-PfFormin1 gives further support to the localization of formin 1 anterior to the rhoptries (Figure 2F, white arrowheads). Close inspection of the three pellicular membranes again suggests a concentration of labeling at the break in the inner membrane complex, possibly associated with the supra-alveolar space lying between the outer plasma membrane and inner membrane complex (Figure 2F, inset).

Since profilin is known to play a key coregulatory role in formin-mediated elongation of actin filaments (Kovar et al., 2003, 2006; Romero et al., 2004), we raised antibodies against recombinant *P. falciparum* profilin (PfPRF) to investigate its localization and timing of expression. PfPRF appears to be present throughout the asexual cycle, peaking in expression coincidently with PfFormin1 (Figure 1B), while dipping at the time of peak expression of PfFormin2 (Figure 1B). Localization of PfPRF within free merozoites is diffuse within the parasite cytosol though concentrating toward the parasite apex, where PfFormin1 is most abundant (Figure 2E). The localization and temporal expression of *P. falciparum* profilin is consistent with it participating in actin polymerization in spite of the fact that PfFormin1 lacks a canonical poly-proline rich FH1 domain (see below) (Figure 1A).

Localization of Formin 1 to the Merozoite-Erythrocyte Tight Junction

The molecular interactions between merozoite and erythrocyte that facilitate cell invasion are believed to localize to an electron dense tight junction formed between the opposing plasma membranes of the parasite and red cell (Miller et al., 1979). Although no components are definitively characterized for this structure in malaria parasites, recent work has identified

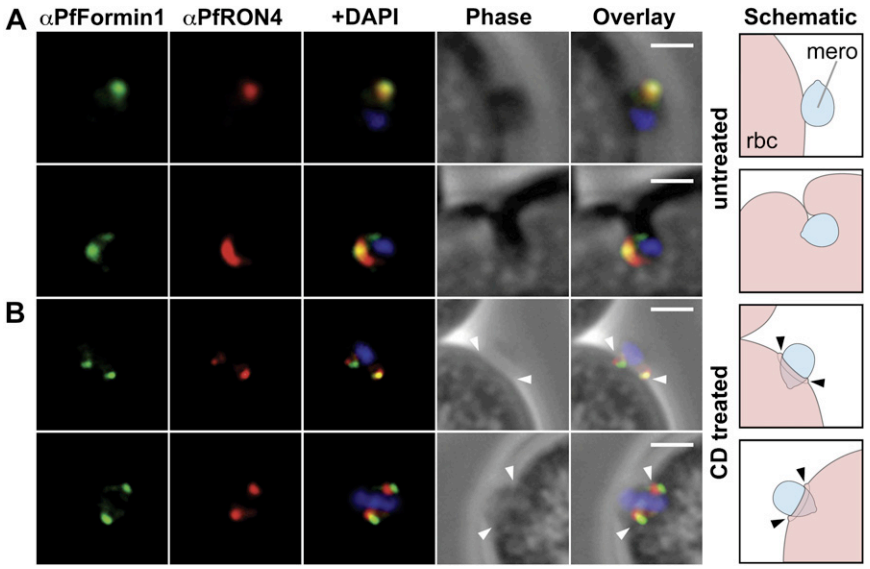

Figure 3. Formin 1 Follows the Moving Tight Junction during Merozoite Invasion of the Erythrocyte

Immunofluorescence and phase contrast micrographs of merozoites during invasion in the absence (A) or presence (B) of cytochalasin D (CD), a drug that inhibits actin polymerization, arresting invasion but not attachment (Miller et al., 1979) (see schematic). Immunofluorescent colocalization of rabbit anti-PfFormin1 with mouse antisera against PfRON4, a rhoptry neck protein that follows the moving tight junction (D.R. and A.F.C., unpublished data). (A) Prior to invasion, PfFormin1 begins at the apical pole coincident with PfRON4. (B) In merozoites arrested midinvasion (CD-treated), PfRON4 is clearly in front of PfFormin1, relative to the direction of tight junction movement (white arrows, black arrow in schematic). Scale bar, 1 μM.

a rhoptry neck protein, TgRON4, in the related apicomplexan parasite *Toxoplasma gondii* (Alexander et al., 2005), which follows the tight (or moving) junction during host cell invasion (Alexander et al., 2005). We investigated the colocalization of the *P. falciparum* ortholog of RON4 (D.R. and A.F.C., unpublished data) and PfFormin1 in merozoites arrested using cytochalasin D, following which merozoites form a tight junction but do not invade (Miller et al., 1979). Prior to invasion, PfFormin1 and PfRON4 colocalize at the apical pole of free merozoites (Figure 3A). However, in the rare event of capturing arrested invasion, fluorescence of both PfFormin1 and PfRON4 appear to split to form two distinct foci (a ring in three dimensions) either side of the merozoite at the interface with the erythrocyte (Figure 3B). This is consistent with their location at the tight junction during merozoite invasion (Figure 3; schematic).

The *Toxoplasma gondii* Formin 1 Ortholog Follows the Active Invasion Motor

Because of the small size (~1.5 μm) and limited viability of merozoites, and given the considerably larger cell size (~7 μm) of *T. gondii* tachyzoites, we investigated whether the formin 1 ortholog in this related parasite follows a similar path. Antibodies against *P. falciparum* formins crossreact with large proteins (>300 kDa) in soluble extracts from free tachyzoites (Figure 1B). The specific crossreactivity of antibodies raised against recombinant PfFormin1 for TgFormin1 was confirmed by immunoblot using extracts from a *T. gondii* line expressing a green fluorescent protein (GFP)-tagged TgFormin1 FH2 domain (Figure S2); the TgFormin1-FH2 domain shares ~50% identity and even greater percentage residue similarity to the FH2 domain of PfFormin1. Immunofluorescence microscopy of free tachyzoites shows TgFormin1 concentrates at the parasite apical pole, in particular associating with the tubulin-rich conoid of the parasite, which can be seen as an extended structure in free tachyzoites (Figure 4A; inset yellow arrow) (Morrissette and Sibley, 2002), and radiating back along the cell periphery following, what appears to be, the early portion of the inner membrane complex (Figure 4A; Movie S1). Furthermore, apical staining can also be seen in the nascent apical complex of daughter cells (Figure 5C; open arrows), which is similar to that seen for *T. gondii* dynein light-chain and calcium-binding proteins recently shown to be associated with the conoid (Hu et al., 2006). It is worth noting that the same study found the formin 1, but not formin 2, ortholog present in conoid-enriched fractions of tachyzoites (Hu et al., 2006). The association of TgFormin1 with the conoid was further investigated in transfectant *Toxoplasma* parasites expressing yellow fluorescence protein (YFP)-tagged α-tubulin (Striepen et al., 2000) (Figure 4B). Formin 1 and α-tubulin clearly colocalize to the conoid in deoxycholate-treated tachyzoites, an extraction process that reveals an intact conoid and microtubules (Hu et al., 2002) (Figure 4B, yellow arrows). Immunoelectron microscopy of free tachyzoites using anti-PfFormin1 serum suggests a close association of TgFormin1 with apical region and outer pellicle of the cell (Figure 4C, white arrows), although there is no close association with a specific cell structure and there is limited (but at a lower percentage) labeling within the central cytosolic region of cells. However, treatment of tachyzoites with *Clostridium septicum* α-toxin (Wichroski et al., 2002), which leads to the selective separation of plasma membrane from the inner membrane complex, clearly shows that the formin 1 protein is associated with the tachyzoite plasma membrane and supra-alveolar space, showing dense staining at the cell periphery (Figure 4D; closed arrow). This is in contrast to the myosin anchor GAP50, which localizes to the outer face of the inner membrane complex (Gaskins et al., 2004) (Figure 4D; open arrow).

We investigated the location of formin 1 during tachyzoite cell invasion. In tachyzoites arrested midinvasion (Kafsack et al., 2004), TgFormin1 progresses down the cell periphery following the moving junction (Figures 5A–5C; white arrows), a structure clearly defined by TgRON4 localization (Alexander et al., 2005) (Figure 5A). The movement of TgFormin1 with RON4 in tachyzoites has significant parallels with *P. falciparum* merozoites during erythrocyte invasion (Figure 3B) and strongly supports a role for formin 1 in regulating actin polymerization during apicomplexan parasite invasion.

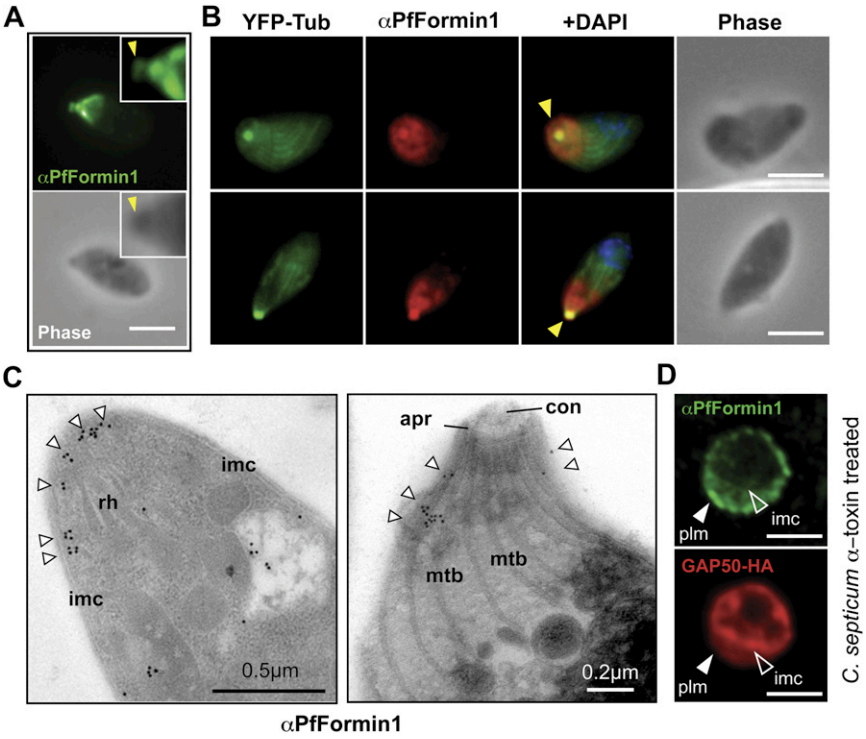

Figure 4. The *Toxoplasma gondii* Formin 1 Ortholog Localizes to the Apical Conoid and Pellicle of Free Tachyzoites

(A) Immunofluorescence and phase contrast micrographs of free *T. gondii* tachyzoites labeled with rabbit PfFormin1 antisera (which recognizes TgFormin1) (Figure 1B; Figure S2). TgFormin1 localizes to the tachyzoite periphery and the apically extended conoid (inset, yellow arrow).

(B) Colocalization of rabbit anti-PfFormin1 with YFP-α-tubulin (Striepen et al., 2000) in 25 mM deoxycholate extracted tachyzoites shows that apical staining of TgFor1 colocalizes with the tubulin-rich conoid (yellow arrow).

(C) Immunoelectron micrographs showing localization of formin 1 in free tachyozites with 10-nm-diameter colloidal gold (white arrowheads). imc, inner membrane complex; rh, rhoptries; apr, apical polar ring; con, remnants of conoid/anterior conoid ring; mtb, subpellicular microtubules.

(D) Localization of rabbit anti-PfFormin1 in *T. gondii* tachyzoites treated with *Clostridium septicum* α-toxin in cells expressing recombinant TgGAP50-HA (C.J.T. and A.F.C., unpublished data). TgFormin1 localizes to the supra-alveolar space underlying the outer plasma membrane (plm, closed arrow), distinct from the inner membrane complex (imc, open arrow), highlighted by the location of GAP50 (Gaskins et al., 2004).

Molecular Modeling of the *P. falciparum* Formin-Actin Interaction

To examine the potential of PfFormin1 and PfFormin2 to nucleate new actin filaments, we undertook molecular modeling of the FH2 domains of both *P. falciparum* formins based on published structures of the FH2 domain of budding yeast formin Bni1p (Otomo et al., 2005; Xu et al., 2004). The FH2 sequences of PfFormin1 and PfFormin2 share ~27% identity with each other and with Bni1p (Otomo et al., 2005; Xu et al., 2004) and share several key residues known to be essential for the interaction of the FH2 dimer with actin (in particular Ile 1431 and a basic residue at 1601) (Otomo et al., 2005) (Figure S3). Furthermore, models of either formin dimer with *P. falciparum* actin demonstrate that the two primary interfaces with the actin monomer,

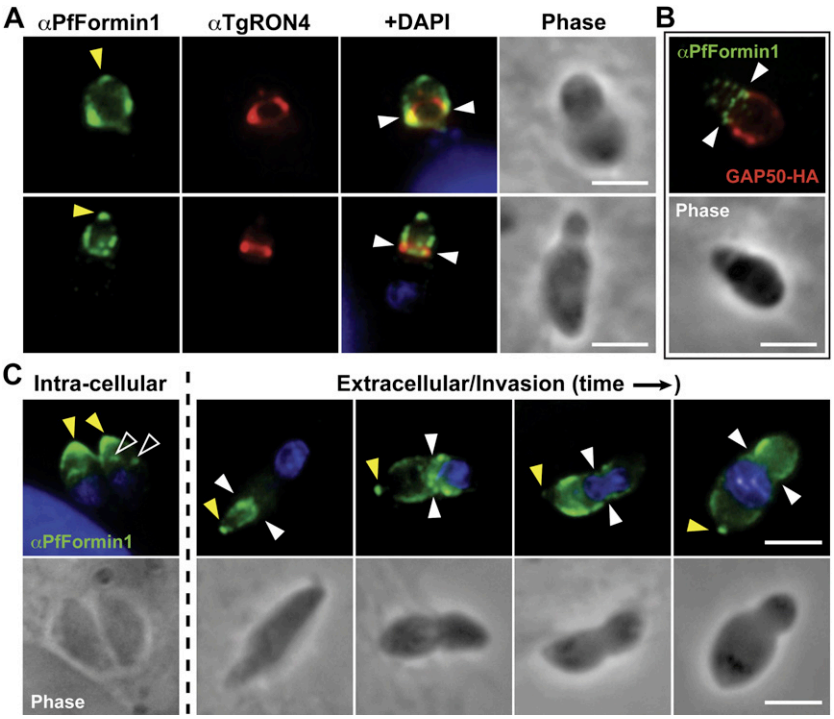

Figure 5. TgFormin1 Localizes to the Moving Junction during Tachyzoite Invasion of Host Cells

Immunofluorescence and phase contrast micrographs of free *T. gondii* tachyzoites arrested midinvasion by buffer exchange. Colocalization of polyclonal rabbit anti-PfFormin1 with (A) an antibody against TgRON4 (Alexander et al., 2005) and (B) with GAP50. TgFormin1 localizes to the moving junction (white arrows), although some remains at the apical pole as the parasite progresses into the host cell (yellow arrow). (C) Time course of tachyzoite invasion pre-host cell rupture and during invasion, probed with anti-PfFormin1. White arrows (closed) indicate progression of the moving junction during invasion. Yellow arrows mark the apical pole inside the host cell. Open arrows indicate conoid development in the developing daughter tachyzoites. DAPI nuclear stain. Scale bar, 5 μM.

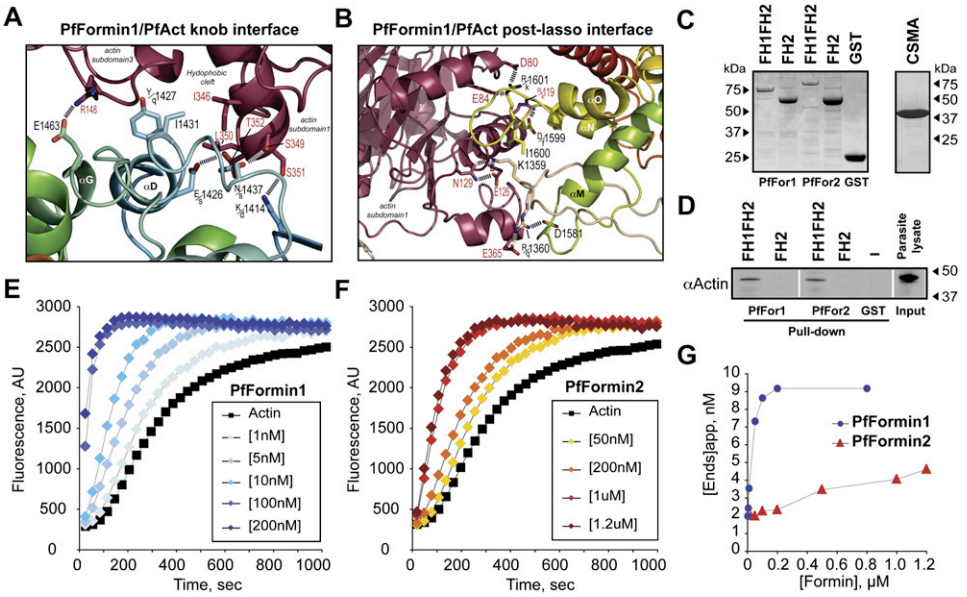

Figure 6. *P. falciparum* Formins Nucleate Actin Polymerization In Vitro

(A and B) Ribbon diagram models of the two main interfaces between the formin dimer of PfFormin1 and *P. falciparum* actin, based on the crystal structure of yeast Bni1p FH2 domain in complex with actin (Otomo et al., 2005). Details show conservation in amino acid properties at two key interfaces with the actin monomer: (A) hydrophobic residues in the knob region—a domain formed by α helices D and G of a single FH2 monomer; and (B) polar residues in the postlasso region—a domain formed by the interaction of α helices M–P of one FH2 monomer and the N terminal portion of the second in the FH2 dimer. Formin residue numbers (black) refer to alignment with Bni1p sequence (Figure S3), while actin residues (red) refer to malaria actin sequence (PlasmoDB ID PFL2215w). Residues marked with a diagonal show the PfFormin1 or PfAct residue (above the line) that differ with Bni1p or vertebrate actin (below the line).

(C) Recombinant or purified proteins used in this study: GST, *P. falciparum* formins 1 (PfFormin1) and 2 (PfFormin2) FH1-FH2 and FH2 domains; and CSMA, chicken skeletal muscle actin.

(D) In vitro pull-down of *P. falciparum* actin from parasite lysates by recombinant GST-PfFormin1 and PfFormin2 FH1-FH2, FH2, or GST alone.

(E–F) Time courses of actin polymerization with (E) PfFormin1-FH1FH2 or (F) PfFormin2-FH1FH2 determined by the fluorescence of pyrenyl-actin. Assembly reactions contained 4 μM Mg-ATP actin (20% pyrenyl labeled) alone or in combination with a range of concentrations of formin GST fusion proteins.

(G) Nucleation efficiency (the concentration of new ends) (Kovar et al., 2003) of PfFormin1-FH1FH2 (blue circles) and PfFormin2-FH1FH2 (red triangles) as determined at half-maximal polymerization over a range (E–F) of formin monomer concentrations.

the knob and postlasso regions (Otomo et al., 2005), show conservation in key hydrophobic and polar residues, respectively (Figures 6A and 6B). Neither *P. falciparum* formin has a clearly defined FH1 domain (Figure 1A) that would be predicted to recruit profilin (Kovar et al., 2003, 2006; Pollard, 2007; Romero et al., 2004), the lack of which appears to be common among apicomplexan formins (data not shown). PfFormin2 has two potential PPPP(L/P)P profilin binding sites, while PfFormin1 has only two pairs of proline residues separated by five other residues (Figure 1A).

Nucleation of Actin by Malaria Parasite Formins In Vitro

Given their potential involvement in invasion, we investigated whether *P. falciparum* formins nucleate actin filaments in vitro. Recombinant proteins comprising truncated and extended PfFormin1 and PfFormin2 FH2 domains were expressed and purified from *E. coli* (Figure 6C). Extended constructs were designed to incorporate the key regions conserved with Bni1p FH2 and include the most extensive poly-proline stretches toward the N-terminus as potential FH1 domains (Figure 1A). To address whether these PfFormin1 and PfFormin2 FH2 domains bind to malaria actin, we undertook pull-down assays of whole parasite lysate using the recombinant GST fusions. Both extended FH1FH2 constructs successfully precipitated parasite actin, though shorter constructs (lacking the essential alpha-helices A and B required for dimerization) (Figure S3) or GST alone did not, supporting an in vivo interaction between parasite formins and actin (Figure 6D). Given that extraction of high quantity (milligram) and purity actin from malaria parasites is practically impossible (Schmitz et al., 2005), we assayed the nucleation potential of the malaria formins with chicken skeletal muscle actin, which despite its divergence, shares key residues in the necessary formin-actin interfaces that are required for nucleation (Figures 6A and 6B and data not shown). PfFormin1-FH1FH2 and PfFormin2-FH1FH2 both stimulated the rate of assembly of bulk samples of chicken actin monomers (measured by increased fluorescence of pyrenyl-actin) (Figures 6E and 6F), demonstrating they are true nucleators. The polymerization rate depended on the concentration of formin (Figures 6E and 6F). Like yeast Bni1pFH1FH2 (Paul and Pollard, 2008), PfFormin1-FH1FH2 strongly stimulates actin assembly at low nanomolar concentrations in the absence of profilin (Figure 6E), while PfFormin2-FH1FH2 was a less potent stimulator (Figure 6F). As predicted, the truncated FH2 domains of either *P. falciparum* formin failed to nucleate actin (data not shown). To calculate the concentration of growing ends across formin concentrations in the bulk polymerization assays and, therefore, measure the nucleation activity of each formin (Kovar et al.,

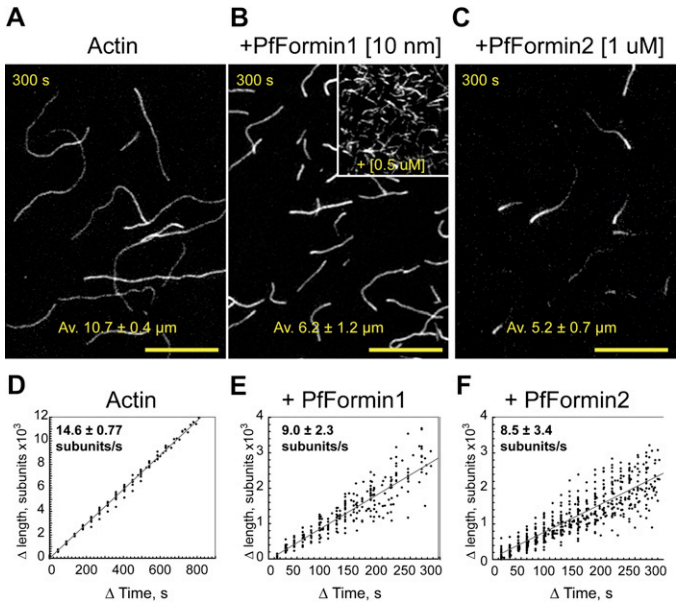

Figure 7. Total Internal Reflection Fluorescence Microscopy of Single Actin Filaments Demonstrates *P. falciparum* Formins Are Barbed-End Nucleators

Nucleation in the presence of Oregon-green-labeled chicken skeletal muscle actin reveals different properties for PfFormin1-FH1FH2 and PfFormin2-FH1FH2.

(A–C) Sample frames from TIRFM taken at ~300 s (postreaction initiation) with average filament lengths given for 10–20 filaments for (A) 1.5 μM actin alone (33% OG-labeled), (B) 1.5 μM actin with 10 nM PfFormin1-FH1FH2 (inset 0.5 μM), and (C) 1.5 μM actin with 1 μM PfFormin2-FH1FH2. Scale bar, 5 μM.

(D–F) Growth of individual actin filament barbed ends observed by TIRFM: (D) actin alone grew at 14.6 ± 0.77 subunits/s (n = 10); (E) actin with 5–10 nM PfFormin1-FH1FH2 grew at 9.0 subunits/s ± 2.3 (n = 20); and (F) actin with 0.2–1 μM PfFormin2-FH1FH2 grew at 8.5 subunits/s ± 3.4 (n = 26).

2003), we used rates of elongation of single filaments measured with microscopy in the presence of either formin (see below). A plot of ends produced versus formin concentration shows that the nucleation activity of PfFormin1-FH1FH2 is much greater than that of PfFormin2-FH1FH2 (Figure 6G). The concentration of ends produced by PfFormin1 plateaus at 9.4 nM because elongation of numerous filaments rapidly depletes the pool of actin subunits available for nucleation.

To distinguish the contributions of nucleation and elongation to actin polymerization stimulated by PfFormin1 and PfFormin2, we used total internal reflection fluorescence microscopy (TIRFM) to measure directly the effect of either recombinant formin on elongation of actin filaments (Kovar et al., 2003) (Figures 7A–7C; Movies S2–S5). Similar to other well-characterized formins (Kovar et al., 2003, 2006; Paul and Pollard, 2008), we found that FH1FH2 constructs of both PfFormin1 and PfFormin2 slowed barbed-end growth (Figures 7E–7F). Elongation rates in the presence of either formin reduced the average barbed-end growth rate from 14.6 ± 0.8 subunits/s for actin alone (Figure 7D) to 9.0 ± 2.3 subunits/s for PfFormin1-FH1FH2 (Figure 7E) and 8.5 ± 3.4 subunits/s for PfFormin2-FH1FH2 (Figure 7F). Filaments growing at rates consistent with actin alone were visible in assays using either formin, suggesting that we observed both free and formin-associated filaments. Moreover, the reduced barbed-end elongation rate with formin is not the result of depletion of the actin monomer pool due to a high number of nucleated ends, but rather, suggests the formin remains bound to the growing barbed end of a nucleated filament—a phenomenon known as processive association (Kovar et al., 2006; Paul and Pollard, 2008).

DISCUSSION

We have shown that malaria formin PfFormin1 is a potent nucleator of filamentous actin, is present at the apical pole of invading merozoites, and comigrates during invasion with the merozoite-erythrocyte moving junction—the predicted location of the actomyosin motor that powers parasite motility. Our results suggest that formin 1 is a key effector of actin filament formation required for successful malaria parasite invasion of the erythrocyte. Furthermore, this role appears to be essential given the failure of repeated attempts, in different malaria parasite strains, to disrupt the function of the formin 1 gene (data not shown). The implication of PfFormin1 in apicomplexan cell locomotion further expands what is already a diverse range of cellular functions that formin-like proteins play in cytoskeletal assembly and organization (Goode and Eck, 2007; Pollard, 2007).

Preliminary in vitro kinetic data for apicomplexan actin suggest that it should form at very low critical concentrations (Sahoo et al., 2006). However, filamentous actin is strikingly absent from apicomplexan parasite cytosol (Bannister and Mitchell, 1995; Dobrowolski et al., 1997; Field et al., 1993; Shaw and Tilney, 1999). The best estimates for the cellular concentration of monomeric actin in *Plasmodium* (Field et al., 1993) and *Toxoplasma* (cited as unpublished data in Sahoo et al., 2006) are well above that required for actin to polymerize in vitro, suggesting tightly controlled regulation of actin filament assembly in vivo. The reduced repertoire of known eukaryotic actin regulators (Baum et al., 2006a) suggests those present play central roles in regulating actin's state. For example, the actin monomer-binding proteins, namely profilin, actin-depolymerizing factor (ADF)/cofilin and Srv2/cyclase-associated protein (Revenu et al., 2004), are likely to play key roles in preventing spontaneous assembly of filaments. However, while these three monomer-binding proteins may be critical in determining availability of actin monomers for polymerization, it is the localization of factors stimulating polymerization that will ultimately determine motor engagement. It is the localization and demonstrated biochemical activity of formin 1, as a stimulator of actin polymerization, that highlight its potential importance to apicomplexan cell motility.

The subcellular concentration of formin 1 at the parasite apex and outer pellicle (Figures 2 and 4) and its localization during invasion (Figures 3 and 5) raises several questions about the molecular processes underlying host cell invasion by apicomplexan parasites. During cell invasion, the arrangement of formin 1 behind RON4 at the moving tight junction suggests RON4 is involved with or follows molecular establishment of the tight junction, which then allows recruitment of the activated motor

complex. However, it is not clear when actin filaments are first initiated and, as such, when formin 1 is actually active. In repeated immunofluorescence microscopy assays with *T. gondii* tachyzoites midinvasion, we consistently observed a proportion of formin 1 fluorescence remaining at the parasite apex past the point of contact with the host cell (Figures 5A and 5C). This observation could be interpreted as evidence that formin 1 stimulates actin polymerization at the parasite apex, after which filaments are translocated by myosin down the length of the parasite pellicle (to the site of the engaged motor complex) carrying with them bound formin. Alternatively, formin 1 may track with the tight junction during its progression, either in association with the motor complex or independently, where it nucleates actin filaments in situ. The first scenario is reminiscent of a model of formin-mediated activation of actin polymerization at the cell tip by the fission yeast formin, For3p (Martin and Chang, 2006). In this model, For3p is transported along microtubules to the cell tip, where it initiates the nucleation of actin cables that are passed rearwards, some carrying a proportion of the bound formin complex with them. Such a model is particularly attractive given the close association we see between formin 1 and components of the microtubular cytoskeleton in merozoites and tachyzoites (Figures 2C and 4A–4C) and the importance these structures play in apicomplexan cell invasion (Fowler et al., 1998; Morrissette and Sibley, 2002). Attempts underway in our laboratory to monitor active formin localization and its association with nascent actin filaments in live invading cells will be able to distinguish between these alternative hypotheses.

In the absence of a full gene knockout, a definitive demonstration of formin 1 function in malaria parasite invasion will depend on development of a system that can disrupt its activity in merozoites, either by expression of a dominant-negative allele or activation of an inducible knockout. Unfortunately, current methods for tetracycline-induced gene regulation in malaria (Meissner et al., 2005) are not robust, resulting in inconsistent levels of expression and, at this time, preclude the investigation of dominant-negative constructs. Furthermore, available vectors for disruption can only carry genes much smaller than either formin (both formins are ~8 kb).

The large size of apicomplexan formins but striking absence of conserved formin autoregulatory domains (Goode and Eck, 2007) raises the potential for identifying novel apicomplexan domains involved in regulation. Furthermore, since Apicomplexa have no orthologs of the small GTPases or other well-characterized upstream effectors of animal or yeast formins (Baum et al., 2006a), the cell factors involved in signaling formin activation in the malaria parasite must involve other, potentially unique, mechanisms. Disruption of these upstream actin effectors should prevent actin polymerization, thereby inactivating the motor and stopping parasite motility/cell invasion. Significantly, since invasion of erythrocytes is central to malaria parasite pathogenicity, the targeting of such actin regulators may be appropriate for development as drug targets against malaria and other apicomplexan parasites.

EXPERIMENTAL PROCEDURES

All chemicals were from Sigma unless noted otherwise.

Parasite Cell Culture and Parasite Invasion Inhibition

P. falciparum (3D7 strain) and *T. gondii* (RH strain) were maintained using standard procedures. *P. falciparum* cultures were grown in human O+ erythrocytes at 4% hematocrit with 0.5% Albumax II (Invitrogen). 3D7 is a cloned line derived from NF54, obtained from the late David Walliker at Edinburgh University, UK. *T. gondii* tachyzoites were propagated in human foreskin fibroblasts (HFF) or Vero cells grown in Dulbecco's modified Eagle's medium (DMEM) with 10% fetal calf serum (GIBCOBRL). *P. falciparum* merozoite invasion was captured following treatment with 0.1 μM cytochalasin D to arrest invasion (Miller et al., 1979). Tachyzoite invasion was captured using a recently described potassium shift protocol (Kafsack et al., 2004).

Recombinant Protein Expression

Expression constructs containing FH2 domains with putative FH1 domains for PfFormin1 (nucleotides 6649–7953) and PfFormin2 (nucleotides 6955–8397) and (predicted nondimerizing) PfFormin1 (nucleotides 6922–7953) and PfFormin2 (nucleotides 7390–8397) FH2 domains alone were generated from 3D7 cDNA and expressed using pGEX4T-1 (Amersham Biosciences). Full length *PfPRF* (amplified from 3D7 cDNA) was expressed as a recombinant hexahistidine fusion using pProEX-HTb (Invitrogen). All proteins were expressed following transformation into *Escherichia coli* BL21 (DE3) strain and, following standard purification protocols, used for mouse and rabbit immunization. All primer sequences are available on request.

Protein Purification and Preparation for Actin Polymerization Assays

GST-formin constructs were purified from bacteria using lysis buffer (50 mM Tris, pH 8.0, 50 mM NaCl, 5 mM EDTA pH 8.0, 1 mM DTT and 0.01% NaN_3) supplemented with Complete protease inhibitor (Roche Applied Science) as described (Kovar et al., 2003). Peak fractions eluted with 100 mM glutathione from a 1.5 ml glutathione-Sepharose column (Amersham Biosciences) were pooled and dialyzed against buffer B50 (10 mM Tris, pH 8.0, 50 mM NaCl, 1 mM EDTA pH 8.0, and 0.01% NaN_3) for 24 hr at 4°C. Dialyzed protein was further purified using a 75 ml linear gradient of 50–500 mM NaCl in Source Q-buffer using a 1 ml Source 15Q column (Amersham Biosciences). Purified FH2 constructs were dialyzed into storage buffer (20 mM HEPES, pH 7.4, 1 mM EDTA, 50 mM NaCl, 10% glycerol, 1 mM DTT, and 0.01% NaN_3) and stored at −80°C. Ca^{2+}-actin was purified from an acetone powder of chicken skeletal muscle as described (MacLean-Fletcher and Pollard, 1980) and stored in Ca^{2+}-G-Buffer (2 mM Tris-HCl, pH 8.0, 0.5 mM $CaCl_2$, 1 mM DTT, and 0.01% NaN_3). Actin was labeled with either Oregon-green (Invitrogen) or pyrenyliodoacetamide (Invitrogen) as described previously (Kovar et al., 2003, 2006).

SDS-PAGE and Immunoblot Analysis

P. falciparum and *T. gondii* tachyzoite parasite pellets were solubilized in 2× SDS loading buffer and separated on 4%–12% (Bis-Tris) or 3%–8% (Tris-Acetate) SDS-NuPAGE gels (Invitrogen) under reducing conditions. Immunoblotting was performed according to standard protocols. Nitrocellulose membranes (0.45 μM; Schleicher and Schuell) were blocked in 10% (w/v) skim milk, 0.1% Tween 20-PBS for 1 hr, and probed with primary antisera in 1% milk, 0.1% Tween 20-PBS for 1 hr (rabbit anti-PfFormin1 [1:300], rabbit anti-PfFormin2 [1:200], rabbit anti-PfPRF [1:300], and rabbit anti-PfAldolase [Baum et al., 2006b] [1:500]). Membranes were washed twice in 0.1% milk, 0.1% Tween 20-PBS for 5 min, and probed with appropriate secondary antibodies (Millipore) for 1 hr. Following five further washes, immunoblots were developed by ECL (Amersham Biosciences).

Immunofluorescence and Transmission Electron Microscopy

For light microscopy, air-dried smears of *P. falciparum* were fixed for 1 min with 100% methanol at −20°C, blocked for 30 min in 3% bovine serum albumin (BSA) in PBS, and incubated with primary antisera in 3% BSA/PBS for 1 hr (rabbit anti-PfFormin1 [1:200]; rabbit anti-PfFormin2 [1:300]; rabbit-anti-PfPRF [1:300]; mouse anti-RAP1 [monoclonal 7H8/50 1:200]; mouse anti-PfFormin1 [1:50]; mouse anti-Actin [monoclonal AC-40, Sigma, 1:100]; mouse anti-tubulin [monoclonal DM1A, Sigma, 1:200]; and mouse anti-PfRON4 [D.R. and A.F.C., unpublished data] [1:200]). Following two 5 min washes in PBS, slides were probed with an appropriate secondary antibody (see below). After four further washes, slides were labeled with DAPI nuclear

stain (Roche Applied Science) at 0.2 μg ml^{-1} in Vectorshield (Vector Labs). Free tachyzoites from culture supernatant or infected host cells were fixed on coverslips in 4% paraformaldehyde (Electron Microscopy Sciences) for 10 min, permeablized in 0.1% Triton X (TX)-100/PBS for 10 min, and blocked in 3% BSA/PBS for 1 hr. Incubation with primary antisera in 3% BSA/PBS was for 1 hr (rabbit anti-PfFormin1 [1:300]; rabbit-anti-TgRON4 [Alexander et al., 2005] [1:1000]; rat anti-HA [monoclonal 3F10, Roche Applied Science, 1:500]), followed by four 5 min washes in PBS and incubation with appropriate secondary antibody for 1 hr (see below). Following four further 5 min washes, coverslips were mounted with DAPI and Vectorshield. Secondary antibodies (Invitrogen) for both parasite assays were goat anti-mouse (Alexa Fluor-488) and -rabbit (Alexa Fluor-594), both at 1:500. Deoxycholate extraction (25 mM) of fixed tachyzoites was carried out in 0.5 mM $MgCl_2$-PBS for 40 min at room temperature in a humidified chamber, followed by blocking and staining, as described above. Dual color fluorescence images were captured using a Carl Zeiss Axioskop 2 microscope (Thornwood) with a PCO SensiCam (Motion Engineering Co.) and Axiovision 3 software (Carl Zeiss). Movie S1 was captured on a Zeiss inverted microscope equipped with AxioVision v4.5 with the raw image stacks deconvolved using the inverse filter algorithm.

Immunolabeling for electron microscopy was performed on 1% glutaraldehyde-fixed schizont or 1% glutaraldehyde, 3% paraformaldehyde-fixed tachyzoite parasite preparations. Schizont sections were a kind gift from S.A. Ralph (University of Melbourne, Victoria, Australia). Tachyzoite parasite preparations were pelleted in low-melting agarose, dehydrated with increasing ethanol concentrations, embedded in Lowicryl-White resin (ProSciTech, Australia), and sectioned on a Leica Ultracut R ultramicrotome (Wetzlar). Sections were blocked with 5% BSA and 0.1% Tween 20/PBS and incubated with either rabbit (*P. falciparum* [1: 20]) or mouse (*T. gondii* [1:500]) primary antisera against PfFormin1 and subsequently labeled with 25 or 10 nm colloidal gold antibodies (Jackson ImmunoResearch, Baltimore, USA). Standard staining with 2% aqueous uranyl-acetate and 5% triple lead preceded observation on a Philips CM120 BioTWIN Transmission Electron Microscope.

Molecular Modeling of Formin-Actin Interactions

Models of the *P. falciparum* formin 1 FH2 dimer were generated by comparative modeling using the MODELER program (http://salilab.org/modeller/modeller.html), employing the *S. cerevisiae* Bni1p FH2 dimer crystal structure (Xu et al., 2004) (PDB number 1UX5) and the crystal structure of the dimer in association with actin (Otomo et al., 2005) (PDB number 1Y64). The alignment used to generate these structures is shown in Figure S3.

Actin Pull-Down

Pull-downs with 100 μg of recombinant FH2, FH1FH2 domains or GST alone, and *P. falciparum* schizont-enriched parasite lysate were carried out using a modified published method (Baum et al., 2006b; Jewett and Sibley, 2003). Schizont-enriched cultures ~40 hr postinvasion were saponin-lysed and washed extensively to remove contaminating erythrocyte material and extracted in 20 pellet volumes of Buffer A (50 mM KCl, 10 mM HEPES [pH 7.5], 1 mM $MgCl_2$, 1 mM EGTA, 2 mM ATP, and 0.2% Tween20 + protease inhibitor cocktail [Roche Applied Science]). Precleared soluble lysate was incubated with the GST fusion overnight at 4°C and pulled down using glutathione agarose beads. Bound proteins were eluted in 2× sample buffer, boiled, and separated by SDS-PAGE. Immunoblots were probed with a mouse monoclonal actin antibody that recognizes PfActin (Field et al., 1993; Patron et al., 2005; Sahoo et al., 2006) (clone C4, Millipore).

Pyrenyl-Actin Polymerization Assays

Actin polymerization was investigated by fluorescence spectroscopy in 96-well flat-bottom plate (Corning) by measuring the change in fluorescence intensity (excitation 362 nm, emission 407 nm) with a Gemini XPS microplate reader (Molecular Devices). Pyrenyl-labeled and unlabeled ATP actin monomers were mixed in Ca^{2+}-G buffer/0.2 mM ATP to obtain a 12 μM stock solution (4 μM final) of 20% pyrenyl-actin. Pyrenyl-actin stock was converted to Mg^{2+} actin by adding 0.1 volume of 10x ME buffer (10 mM $MgCl_2$, 10 mM EGTA) for 2 min at 25°C in the presence of Antifoam 204 at 5 parts/10^5. Varying concentrations of recombinant formin in Mg^{2+}-G buffer (as Ca^{2+}-G-buffer but with 0.1 mM $MgCl_2$) and 0.1 volume (final reaction volume) of 10× KMEI (500 mM KCl, 10 mM $MgCl_2$, 10 mM EGTA, and 100 mM imidazole, pH 7.0) were assembled separately. The reaction was started by adding the protein/buffer mix to the actin stock, and assayed immediately. Pyrenyl-actin fluorescence was monitored every 5–10 s. Time between mixing of final components and start of fluorometer data collection averaged between 15 and 25 s.

Total Internal Reflection Fluorescence Microscopy

Flow cells were assembled using ESCO Superfrost glass slides (Erie Scientific), cleaned as described (Kuhn and Pollard, 2005), and single 22 × 50 mm coverslips (Fisherbrand) mounted with Parafilm to create a 6 mm flow channel. Prior to TIRFM assays, 10–15 μl of 200 nM NEM-myosin from skeletal muscle was passed one to two times through flow cells, allowed to adhere to the slide for 1 min, and washed twice with 10 μl of HS-TBS (0.6 M NaCl, 50 mM Tris-HCl, pH 7.5) and once with 10 μl of Super-Block (Pierce). These were stored in a humid chamber and used within 1 hr of preparation or kept at 4°C for use within 2 days.

Prior to each assay, a fresh flow cell was flushed with 1× TIRF Buffer (9.6 mM imidazole, pH 7.0, 48 mM KCl, 0.96 mM $MgCl_2$, 0.96 mM EGTA, 48 mM DTT, 0.19 mM ATP, 14.4 mM glucose, 19.2 mg/ml catalase, 96 mg/ml glucose oxidase, 0.48% methylcellulose [4000 cP at 2%], 0.19% BSA). TIRF microscopy assays were performed using Oregon green-labeled ATP actin (30% labeled) converted from Ca^{2+}-ATP actin to Mg^{2+}-ATP actin by addition of 0.2 volumes of 1 mM EGTA and 0.25 mM $MgCl_2$. Polymerization was initiated by adding 2× TIRF Buffer mixed with formin (supplemented with storage buffer [see above] to give appropriate final polypeptide concentration) to the Mg^{2+}-ATP actin. The reactions were transferred to a mounted flow cell with imaging initiated as soon as filaments appeared (2–5 min, depending on flow and polymerization rates). Images of fluorescent actin filaments excited by total internal reflection were collected at 10–15 s intervals with a Hamamatsu C4742-95 CCD camera (Orca-ER) on an Olympus IX-70 microscope. Images were acquired with the Olympus Metamorph Imaging software and processed with IMAGEJ software (National Institute of Health, http://rsb.info.nih.gov/ij).

SUPPLEMENTAL DATA

The Supplemental Data include three supplemental figures and five supplemental movies and can be found with this article online at http://www.cellhostandmicrobe.com/cgi/content/full/3/3/188/DC1/.

ACKNOWLEDGMENTS

We are grateful to J.I. Rood, D. Lyras, and C.L. Kennedy (Monash University, Victoria, Australia) for providing *C. septicum* α-toxin; J.C. Boothroyd (Stanford University, CA, USA) for providing antibodies against TgRON4; D.S. Roos (University of Pennsylvania, PA, USA) for providing the YFP-α tubulin plasmid; S.A. Ralph (University of Melbourne, Victoria, Australia) for *P. falciparum* schizont sections for immunolabeling; and the Red Cross Blood Service (Melbourne, Australia) for supply of red cells. We thank A. Downs for technical advice and B. Baum for critical reading of the manuscript. Biochemical work was undertaken at Yale University and made possible by grants from the Australian Research Council/National Health and Medical Research Council Network for Parasitology, the Australian Academy of Science, and the Human Frontier Science Program. Parasite work was undertaken at the Walter and Eliza Hall Institute and funded by the NHMRC and the Wellcome Trust. J.B. is funded by a Career Development Award from the NHMRC. A.F.C. is a Howard Hughes International Research Scholar and an NHMRC Australia Fellow. Experiments were designed and data analyzed and interpreted by J.B., C.J.T., A.P., T.D.P., and A.F.C. Parasite transfection, immunoblot, and fluorescence microscopy analyses were performed by J.B. and C.J.T. Recombinant protein and biochemical assays (pyrenyl-actin and TIRF microscopy) were performed by J.B. and A.P. Electron microscopy was carried out by M.R., S.B.G., and J.B. Molecular modeling of actin-formin interactions were performed and analyzed by B.J.S. and J.B. Antibodies against PfRON4 were raised, tested, and validated by D.R. The manuscript was written by J.B., T.D.P., and A.F.C. All authors discussed the results and commented on the manuscript.

Received: October 2, 2007
Revised: January 22, 2008
Accepted: February 18, 2008
Published: March 12, 2008

REFERENCES

Alexander, D.L., Mital, J., Ward, G.E., Bradley, P., and Boothroyd, J.C. (2005). Identification of the Moving Junction Complex of Toxoplasma gondii: A Collaboration between Distinct Secretory Organelles. PLoS Pathog. *1*, e17.

Bannister, L.H., and Mitchell, G.H. (1995). The role of the cytoskeleton in Plasmodium falciparum merozoite biology: An electron-microscopic view. Ann. Trop. Med. Parasitol. *89*, 105–111.

Baum, J., Papenfuss, A.T., Baum, B., Speed, T.P., and Cowman, A.F. (2006a). Regulation of apicomplexan actin-based motility. Nat. Rev. Microbiol. *4*, 621–628.

Baum, J., Richard, D., Healer, J., Rug, M., Krnajski, Z., Gilberger, T.W., Green, J.L., Holder, A.A., and Cowman, A.F. (2006b). A conserved molecular motor drives cell invasion and gliding motility across malaria lifecycle stages and other apicomplexan parasites. J. Biol. Chem. *281*, 5197–5208.

Dobrowolski, J.M., Niesman, I.R., and Sibley, L.D. (1997). Actin in the parasite Toxoplasma gondii is encoded by a single copy gene, ACT1 and exists primarily in a globular form. Cell Motil. Cytoskeleton *37*, 253–262.

Dobrowolski, J.M., and Sibley, L.D. (1996). Toxoplasma invasion of mammalian cells is powered by the actin cytoskeleton of the parasite. Cell *84*, 933–939.

Field, S.J., Pinder, J.C., Clough, B., Dluzewski, A.R., Wilson, R.J., and Gratzer, W.B. (1993). Actin in the merozoite of the malaria parasite, Plasmodium falciparum. Cell Motil. Cytoskeleton *25*, 43–48.

Foth, B.J., Goedecke, M.C., and Soldati, D. (2006). New insights into myosin evolution and classification. Proc. Natl. Acad. Sci. USA *103*, 3681–3686.

Fowler, R.E., Fookes, R.E., Lavin, F., Bannister, L.H., and Mitchell, G.H. (1998). Microtubules in Plasmodium falciparum merozoites and their importance for invasion of erythrocytes. Parasitology *117*, 425–433.

Gaskins, E., Gilk, S., DeVore, N., Mann, T., Ward, G., and Beckers, C. (2004). Identification of the membrane receptor of a class XIV myosin in Toxoplasma gondii. J. Cell Biol. *165*, 383–393.

Goode, B.L., and Eck, M.J. (2007). Mechanism and Function of Formins in Control of Actin Assembly. Annu. Rev. Biochem. *76*, 593–627.

Higashida, C., Miyoshi, T., Fujita, A., Oceguera-Yanez, F., Monypenny, J., Andou, Y., Narumiya, S., and Watanabe, N. (2004). Actin polymerization-driven molecular movement of mDia1 in living cells. Science *303*, 2007–2010.

Higgs, H.N., and Peterson, K.J. (2005). Phylogenetic analysis of the formin homology 2 domain. Mol. Biol. Cell *16*, 1–13.

Hu, K., Johnson, J., Florens, L., Fraunholz, M., Suravajjala, S., DiLullo, C., Yates, J., Roos, D.S., and Murray, J.M. (2006). Cytoskeletal components of an invasion machine–the apical complex of Toxoplasma gondii. PLoS Pathog. *2*, e13.

Hu, K., Roos, D.S., and Murray, J.M. (2002). A novel polymer of tubulin forms the conoid of Toxoplasma gondii. J. Cell Biol. *156*, 1039–1050.

Jewett, T.J., and Sibley, L.D. (2003). Aldolase forms a bridge between cell surface adhesins and the actin cytoskeleton in apicomplexan parasites. Mol. Cell *11*, 885–894.

Kafsack, B.F., Beckers, C., and Carruthers, V.B. (2004). Synchronous invasion of host cells by Toxoplasma gondii. Mol. Biochem. Parasitol. *136*, 309–311.

Kovar, D.R., Harris, E.S., Mahaffy, R., Higgs, H.N., and Pollard, T.D. (2006). Control of the assembly of ATP- and ADP-actin by formins and profilin. Cell *124*, 423–435.

Kovar, D.R., Kuhn, J.R., Tichy, A.L., and Pollard, T.D. (2003). The fission yeast cytokinesis formin Cdc12p is a barbed end actin filament capping protein gated by profilin. J. Cell Biol. *161*, 875–887.

Kuhn, J.R., and Pollard, T.D. (2005). Real-time measurements of actin filament polymerization by total internal reflection fluorescence microscopy. Biophys. J. *88*, 1387–1402.

Le Roch, K.G., Zhou, Y., Blair, P.L., Grainger, M., Moch, J.K., Haynes, J.D., De La Vega, P., Holder, A.A., Batalov, S., Carucci, D.J., et al. (2003). Discovery of gene function by expression profiling of the malaria parasite life cycle. Science *301*, 1503–1508.

MacLean-Fletcher, S., and Pollard, T.D. (1980). Identification of a factor in conventional muscle actin preparations which inhibits actin filament self-association. Biochem. Biophys. Res. Commun. *96*, 18–27.

Martin, S.G., and Chang, F. (2006). Dynamics of the formin for3p in actin cable assembly. Curr. Biol. *16*, 1161–1170.

Meissner, M., Krejany, E., Gilson, P.R., de Koning-Ward, T.F., Soldati, D., and Crabb, B.S. (2005). Tetracycline analogue-regulated transgene expression in Plasmodium falciparum blood stages using Toxoplasma gondii transactivators. Proc. Natl. Acad. Sci. USA *102*, 2980–2985.

Meissner, M., Schluter, D., and Soldati, D. (2002). Role of Toxoplasma gondii myosin A in powering parasite gliding and host cell invasion. Science *298*, 837–840.

Michelot, A., Guerin, C., Huang, S., Ingouff, M., Richard, S., Rodiuc, N., Staiger, C.J., and Blanchoin, L. (2005). The formin homology 1 domain modulates the actin nucleation and bundling activity of Arabidopsis FORMIN1. Plant Cell *17*, 2296–2313.

Miller, L.H., Aikawa, M., Johnson, J.G., and Shiroishi, T. (1979). Interaction between cytochalasin B-treated malarial parasites and erythrocytes. Attachment and junction formation. J. Exp. Med. *149*, 172–184.

Mizuno, Y., Makioka, A., Kawazu, S., Kano, S., Kawai, S., Akaki, M., Aikawa, M., and Ohtomo, H. (2002). Effect of jasplakinolide on the growth, invasion, and actin cytoskeleton of Plasmodium falciparum. Parasitol. Res. *88*, 844–848.

Morrissette, N.S., and Sibley, L.D. (2002). Cytoskeleton of apicomplexan parasites. Microbiol. Mol. Biol. Rev. *66*, 21–38.

Otomo, T., Tomchick, D.R., Otomo, C., Panchal, S.C., Machius, M., and Rosen, M.K. (2005). Structural basis of actin filament nucleation and processive capping by a formin homology 2 domain. Nature *433*, 488–494.

Patron, S.A., Mondragon, M., Gonzalez, S., Ambrosio, J.R., Guerrero, B.A., and Mondragon, R. (2005). Identification and purification of actin from the subpellicular network of Toxoplasma gondii tachyzoites. Int. J. Parasitol. *35*, 883–894.

Paul, A., and Pollard, T. (2008). The Role of the FH1 Domain and Profilin in Formin-Mediated Actin-Filament Elongation and Nucleation. Curr. Biol. *18*, 9–19. Published online December 20, 2007.

Pinder, J.C., Fowler, R.E., Dluzewski, A.R., Bannister, L.H., Lavin, F.M., Mitchell, G.H., Wilson, R.J., and Gratzer, W.B. (1998). Actomyosin motor in the merozoite of the malaria parasite, Plasmodium falciparum: Implications for red cell invasion. J. Cell Sci. *111*, 1831–1839.

Pollard, T.D. (2007). Regulation of actin filament assembly by Arp2/3 complex and formins. Annu. Rev. Biophys. Biomol. Struct. *36*, 451–477.

Raibaud, A., Lupetti, P., Paul, R.E., Mercati, D., Brey, P.T., Sinden, R.E., Heuser, J.E., and Dallai, R. (2001). Cryofracture electron microscopy of the ookinete pellicle of Plasmodium gallinaceum reveals the existence of novel pores in the alveolar membranes. J. Struct. Biol. *135*, 47–57.

Revenu, C., Athman, R., Robine, S., and Louvard, D. (2004). The co-workers of actin filaments: From cell structures to signals. Nat. Rev. Mol. Cell Biol. *5*, 635–646.

Romero, S., Le Clainche, C., Didry, D., Egile, C., Pantaloni, D., and Carlier, M.F. (2004). Formin is a processive motor that requires profilin to accelerate actin assembly and associated ATP hydrolysis. Cell *119*, 419–429.

Sagot, I., Klee, S.K., and Pellman, D. (2002). Yeast formins regulate cell polarity by controlling the assembly of actin cables. Nat. Cell Biol. *4*, 42–50.

Sahoo, N., Beatty, W., Heuser, J., Sept, D., and Sibley, L.D. (2006). Unusual kinetic and structural properties control rapid assembly and turnover of actin in the parasite Toxoplasma gondii. Mol. Biol. Cell *17*, 895–906.

Schmitz, S., Grainger, M., Howell, S., Calder, L.J., Gaeb, M., Pinder, J.C., Holder, A.A., and Veigel, C. (2005). Malaria parasite actin filaments are very short. J. Mol. Biol. *349*, 113–125.

Schuler, H., Mueller, A.K., and Matuschewski, K. (2005). Unusual properties of Plasmodium falciparum actin: New insights into microfilament dynamics of apicomplexan parasites. FEBS Lett. *579*, 655–660.

Shaw, M.K., and Tilney, L.G. (1999). Induction of an acrosomal process in Toxoplasma gondii: Visualization of actin filaments in a protozoan parasite. Proc. Natl. Acad. Sci. USA *96*, 9095–9099.

Striepen, B., Crawford, M.J., Shaw, M.K., Tilney, L.G., Seeber, F., and Roos, D.S. (2000). The plastid of Toxoplasma gondii is divided by association with the centrosomes. J. Cell Biol. *151*, 1423–1434.

Wetzel, D.M., Hakansson, S., Hu, K., Roos, D., and Sibley, L.D. (2003). Actin filament polymerization regulates gliding motility by apicomplexan parasites. Mol. Biol. Cell *14*, 396–406.

Wichroski, M.J., Melton, J.A., Donahue, C.G., Tweten, R.K., and Ward, G.E. (2002). Clostridium septicum alpha-toxin is active against the parasitic protozoan Toxoplasma gondii and targets members of the SAG family of glycosylphosphatidylinositol-anchored surface proteins. Infect. Immun. *70*, 4353–4361.

Xu, Y., Moseley, J.B., Sagot, I., Poy, F., Pellman, D., Goode, B.L., and Eck, M.J. (2004). Crystal structures of a Formin Homology-2 domain reveal a tethered dimer architecture. Cell *116*, 711–723.